

## Textural analysis of a microcrystalline quartz using X-Ray and Electron Backscatter Diffraction (EBSD) techniques

Daniel Chateigner<sup>1</sup>, Gianfranco Camana<sup>2</sup>, and Patrick Trimby<sup>3</sup>

<sup>1</sup>Laboratoire Cristallographie et Science des Matériaux – ISMRA, 6 Bd. Maréchal Juin,  
F-14050 Caen, France

<sup>2</sup>Dipartimento di Ingegneria dei Materiali, Univeristà di Trento, Italy

<sup>3</sup> HKL Technology, Hobro, Denmark

**Keywords:** Textural analysis, quartz, X-Ray diffraction, EBSD, pole figures, grid-work texture

**Abstract.** An unusual microcrystalline quartz texture has been recognized in the investigation of pervasively silicified ore-bearing horizons occurring in the uppermost part of carbonate platform sequences of different ages (from Precambrian to Mesozoic) and of different geotectonic settings. This peculiar texture has been labeled “grid-work texture”, and derives only by a rather fast and preferred crystallization of quartz on the pre-existing morphological faces of other developed quartz crystals. The 001 pole figures obtained by X-ray textural analysis describe this grid-work texture as constituted by two components of orientation: one component at about 35° from the normal to the surface of the sample and a second orientation component having the c axes oriented at about 75° from the normal to the surface of the sample. Textural maps and parameters obtained by EBSD found very similar components of orientation highlighting as 30-40° and 70-80° misorientations are very common; moreover they allowed to establish as many of the quartz crystals are characterized by Dauphiné Twin boundaries.

### Introduction

In this paper will be showed the good agreement of the textural parameters of a microcrystalline quartz (average grain size 50 µm) obtained by X-Ray and Electron Backscatter Diffraction (EBSD) techniques and how they provide textural information at different scales. This type of microcrystalline texture labeled “grid-work texture” derives from pervasively silicified and variously mineralised horizons (Siliceous Crust Type, SCT) linked to carbonate platform sequences of different ages (from Proterozoic to Tertiary) and geological setting (major occurrences observed: Alps, Sardinia, Calabria, French and Spanish Pyrenees, Cantabric Chain, China, Brazil) [1,2,3,4].

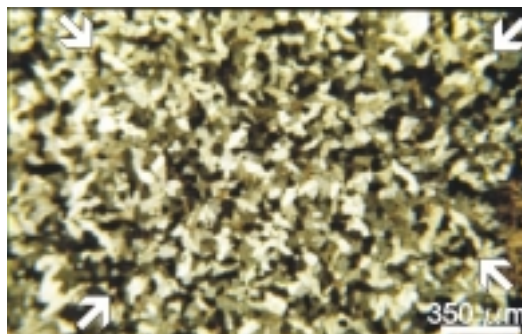


Fig.°1: Microscopy of the grid-work texture in SCT horizons obtained with crossed nicols inserted. White arrows highlight the two sub-perpendicular directions of elongated quartz grains.

The major characteristic of SCT horizons is the almost total silicification of an original polymictic conglomerate-breccia mainly constituted by carbonate fragments and rare siliciclastic rocks developed on palaeokarst landscapes. Geological, structural, compositional and geochemical

parameters indicate that the most likely source of silica in the case of the SCT horizons are basinal sedimentary sequences. The grid-work texture is particularly evident when observed at the optical microscope. Under such conditions the quartz crystals describe a grid pattern, with two populations of elongated grains arranged in sub-perpendicular directions (Fig.°1). By rotating the plate of the microscope of 45° the iso-oriented elongated quartz grains switch alternatively from extinction position (black) to light positions (white). Other less elongated grains appear blackish and they don't change by rotating the plate of the microscope.

### Experimental Conditions

A CPS120 curved position sensitive detector from Inel-S.A. and a Huber four-circle goniometer, using copper  $K_{\alpha 12}$  radiation in the reflection mode on flat specimen, have been used for X-Ray texture analysis. The used methodology, which allows to collect simultaneously all the pole figures in the range  $0 < 2\theta < 120^\circ$  for each sample orientation, has been described elsewhere in details [5]. For microcrystalline quartz (space group  $P3_221$ ,  $a = 4.912 \text{ \AA}$ ,  $c = 5.404 \text{ \AA}$ ), we acquired all the diagrams with a constant incidence angle  $\omega = 13^\circ$ , that is almost the half of the angle at which the 101 peak occurs, which in our optics setup gives an irradiated area on the sample of approximately  $1 \times 5 \text{ mm}^2$ . This area was further increased to  $5 \times 5 \text{ mm}^2$  by oscillating the sample during the acquisition, in order to probe a larger number of grains. In this configuration, we estimate the number of irradiated grains to be of the order of  $10^4$ . The tilt angle ( $\chi$ ) was varied from 0 to  $70^\circ$  and the azimuthal angle ( $\phi$ ) from 0 to  $355^\circ$ , both in steps of  $5^\circ$ . A counting time of 60 seconds for each diagram provided enough intensity to reliably measure most of the diffracted peaks in the low angle region. The ODF refinement was operated on the 7 lower d-spacing quartz peaks, using the WIMV algorithm of Beartex [5]. We obtained RP factors of RP0 ranging from 3.02 to 11.34% and of RP1 from 3 to 9.06%, with a texture strength of  $F^2$  from 1.24 to 3.08  $\text{mrd}^2$ .

A W-filament JEOL 840 SEM, equipped with the HKL Technology CHANNEL 5 EBSD software, has been used to perform an automated EBSD analysis on a SCT microcrystalline quartz sample. A grid of 154 by 115 points with a spacing of  $2.5 \mu\text{m}$  between each point was used, collecting and, where possible, indexing each point. The analysis took  $1\frac{1}{4}$  hours to perform (approximately 4 points per second).

### X-Ray textural analysis

The recalculated  $\{001\}$  and  $\{100\}$  pole figures have found very similar texture patterns for all the samples analyzed. All the observed texture patterns can be summarized by the representative sample B1 which exhibits all texture components (Fig.°2). The  $\{001\}$  pole figure, characterizing the c-axes distribution, exhibit two main components of orientation (labeled components A and B). The first component A is located at about  $35^\circ$  from the normal to the surface of the sample, while the second component B is more inclined, from  $60^\circ$  to  $85^\circ$  from the normal, and distributed on a girdle. One can observe that this  $\{001\}$  component corresponds to localized poles in the  $\{100\}$  pole figures, distributed around the expected place for a single crystal, at  $60^\circ$  from one another and up to  $35^\circ$  from the equatorial plane. This component of orientation is due to quartz grains cut sub-perpendicularly with respect to the c axis, which remain almost constantly extinct at the microscope (i.e. blackish in Fig.°1) upon sample rotation.

The second orientation component B, is related to quartz crystals having the c axes oriented at about  $75^\circ$  from the normal to the surface of the samples. The 001 poles for this component are distributed on a girdle which defines a fiber-like texture having a fiber axis inclined by around  $30^\circ$  from the sample's normal. This component of orientation corresponds to quartz grains cut sub-longitudinally with respect to the c axis, which appear as elongated quartz grains at the microscope switching alternatively from extinction to light position (Fig.°1).

The texture components A and B do not change if we analyze parallel sections cut at different locations in the bulk specimen, and therefore they represent a truly three-dimensional feature of the investigated microcrystalline quartz samples.

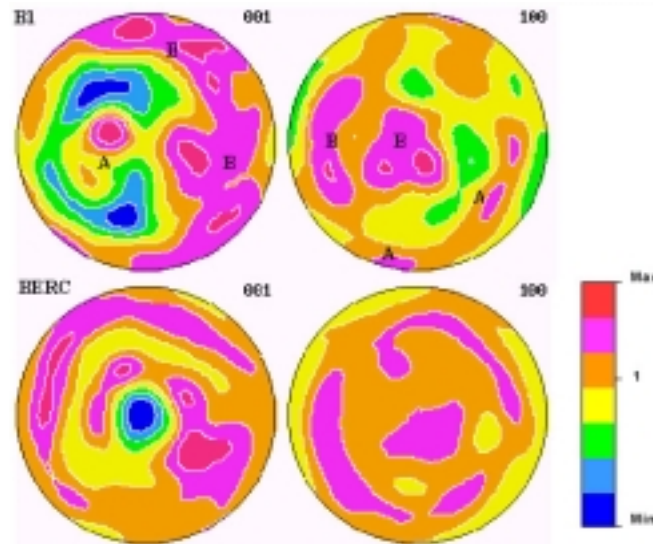


Fig. 2: Recalculated 001 and 100 pole figures for samples B1 and BERG. Texture components A and B are indicated for sample B1.

### EBSD analysis

Although only 55% of the points were successfully indexed (in part due to the abundance of pores, but also due to the poor patterns quality in many areas), careful extrapolation of the data results in a reliable representation of the microstructure. The pole figures (Fig.3) show that there is a weak c-axis maximum parallel to the normal to the surface (center of the {001} pole figure) and few isolated maxima at a high angle (60 to 75°) from the normal. As observed with x-rays, the texture is three dimensionally present.

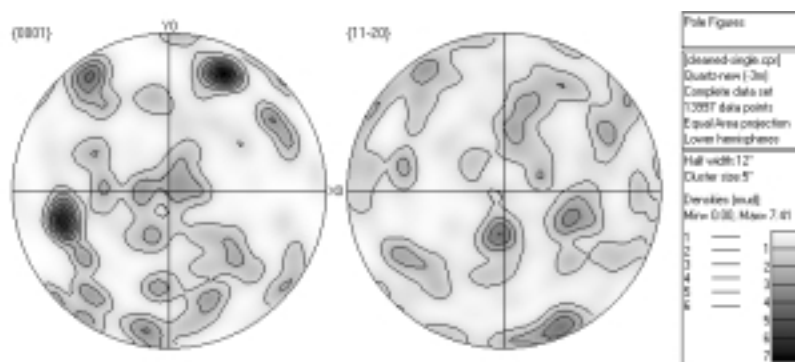


Fig. 3: C-axis and a-axis pole figures from an EBSD orientation map.

The distribution of misorientation boundary frequencies is shown in Fig. 4. Low angle ( $< 6^\circ$ ) and Dauphiné Twin-like (prominent peak at  $60^\circ$ ) boundaries are the most abundant. Other minor peaks are present at  $70-75^\circ$  and at  $85^\circ$  misorientations. The abundance of low angle boundaries indicates that there may be significant intra-granular deformation. As a matter of fact it has been possible to recognize the progressive change in orientation within single grains. Some transects have shown changes in misorientation progressing up to  $6^\circ$  across the length of the grain. This fact is indicative

of significant deformation accompanied by a lack of recovery (to be expected at the original low pressure and temperature conditions characterizing the samples).

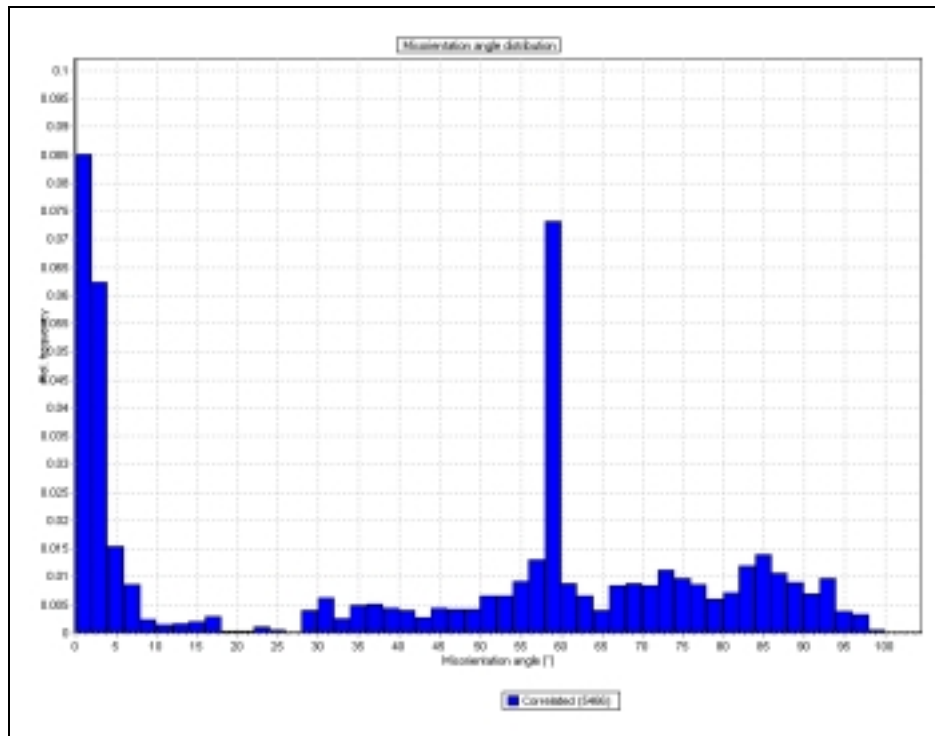


Fig.°4: Typical Boundary misorientation frequency distribution

X-ray textural analysis suggested that c-axes may be preferentially oriented perpendicular to common crystal faces, hereby producing misorientations of about  $35^\circ$  and  $75^\circ$ . The EBSD quality map of Fig.°5 highlights that such boundaries are very common.

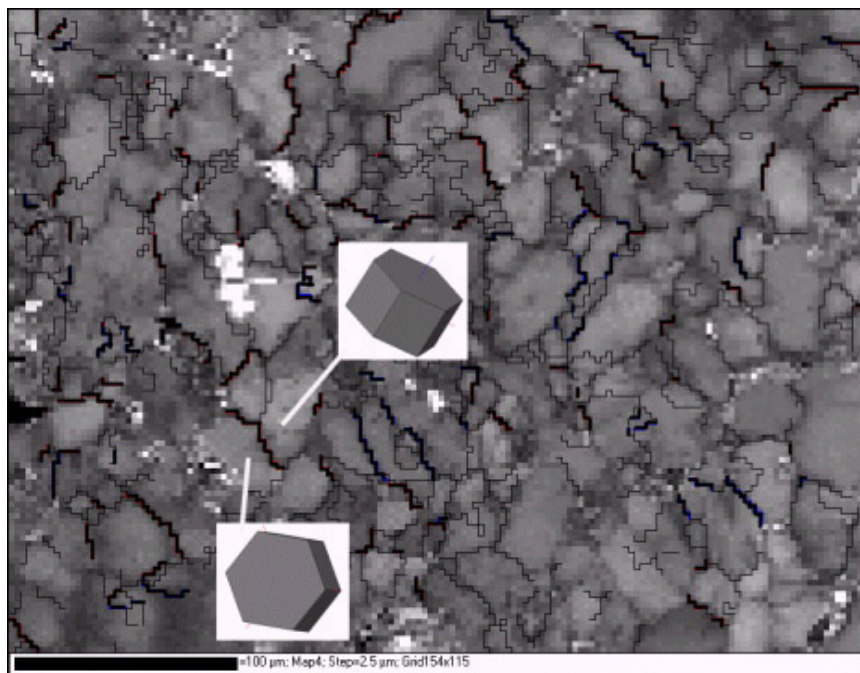


Fig.°5: EBSD quality map with the  $30\text{-}40^\circ$  and  $70\text{-}80^\circ$  boundaries highlighted (bold lines). The 3D simulations show the crystals orientations on each side of one such boundary

The simulated 3D crystal orientation on each side of such a boundary has been marked: this shows that c-axis orientation in the lower grain is close to perpendicular to the prism m face of the upper grain.

## Discussion-Conclusion

The results shown here highlight the complementary nature of textural approaches that are X-Ray and EBSD techniques. X-Ray diffraction provides textural information, which are an average value for the whole sampled area, typically comprising thousands of grains [6] ( $10^4$  grains in our case). Since all the peak profiles were used in the x-ray ODF refinements, also those crystallites that typically provide non-indexable EBSD patterns are taken into account. This may explain the little differences observed between x-rays and EBSD approaches in our case, which makes the former methodology easier to use for a global determination of the texture. Of course, no information neither at the scale of the single grains nor on misorientations are provided by X-ray analysis. In our case, EBSD analysis confirms X-Ray data finding c-axis maxima parallel (z-direction; component A) and inclined (component B) from the surface normal (Fig. 3). Moreover, the analysis of the distribution of misorientation boundaries highlights the low angle ( $< 6^\circ$ ) and Dauphiné Twin boundaries (peak at  $60^\circ$ ). The presence of a large amount of Dauphiné Twins may indicate new helpful features for understanding and defining both the palaeoenvironments and mechanisms under which the grid-work texture of quartz develops.

Because of the geological, mineralogical and geochemical constraints of the SCT horizons, which represent a new type within the heterogeneous group of siliceous sedimentary rocks [2,3], we tentatively support the following model to explain the textural characteristics of microcrystalline SCT quartz. We consider a mechanism involving a rather fast nucleation of quartz on the pre-existing morphological faces of other developed quartz crystals such as the prism  $m \{100\}$ , the positive and negative rhombohedra  $r \{101\}$  and  $z \{011\}$ . All of these forms are listed as universal or very common of quartz. Some of the interfacial angles of interest are for example:  $[101] \wedge [011] = 76,42^\circ$ , or  $[100] \wedge [101] = 38,21^\circ$ . This mechanism does not require large chemical, temperature or pressure gradients and it may therefore be consistent with the observed three-dimensionality of the grid-work texture and the homogeneous spatial distribution of the texture components in the samples. The proposed mechanism may as well be applied to minerals other than quartz, and indeed there are examples in literature where similar textures have been observed in rocks. One striking case is the so called “stellate” texture of calcite observed in the carbonatic cement matrix of Permian hiatus beds [7].

## Acknowledgements

This work has been funded by the European Union project under the Growth program (G6RD-CT99-00169) ESQUI.

## References

- [1] F. Rodeghiero, I. Fanlo, I. Subias, C. Fernandez-Nieto and L. Brigo: *Acta Geologica Hispanica* Vol. 30 (1996), 69-81.
- [2] G. Camana: Ph. D. Thesis Milano University (1999), 182 pp.
- [3] L. Brigo, G. Camana, F. Rodeghiero and R. Potenza: *Ore Geology Reviews* Vol. 17 (2001), 199-214.
- [4] G. Camana, D. Chateigner, M. Zucali and G. Artioli: *American Mineralogist* (2002) In press.
- [5] J. Ricote, D. Chateigner, L. Pardo, M. Algueró, J. Mendiola and M.L. Calzada: *Ferroelectrics* Vol. 241 (2000), 167-174.
- [5] Wenk H.-R., Matthies S., Donovan J., Chateigner D. (1998). *J. of Appl. Cryst.* **31**, 262-269.
- [6] V. Randle, O. Engler: *Texture analysis - Macrotecture, Microtexture & Orientation Mapping* (Gordon and Breach Science Publishers, 2000).

- [7] W. Wetzel, A. Allia: *Journal of Sedimentary Geology* Vol 70 (2000), 170-180.